A new drop weight impact machine for studying the fracture behaviour of structural concrete

X. X. Zhang[1,2], G. Ruiz[1] & R. C. Yu[1]
[1]*E.T.S. de Ingenieros de Caminos, Canales y Puertos, Universidad de Castilla-La Mancha, Spain*
[2]*Harbin Engineering University, China*

Abstract

This paper describes the main characteristics of a new drop weight impact machine that has been specifically designed for studying the dynamic mechanical behaviour of structural concrete samples. Such equipment has been used to generate simple and measurable fracture processes under moderate to fast loading rates, as opposed to blast chambers, which produce complicated crack patterns that are difficult to analyze. The machine consists of two main parts, the mechanical structure and the data acquisition system. The former is just a hammer, guided by two robust columns, which can impact the specimen with energy up to 7860 J. The latter consists of piezoelectric force sensors, accelerometers and an optical fibre photoelectric sensor plus oscilloscopes and signal conditioners. The paper also presents the results of some preliminary tests that show the sensitivity of the work of fracture to the loading rate.

Keywords: drop weight impact machine, concrete, work of fracture.

1 Introduction

The response of concrete to dynamic loading is of interest in a variety of civilian and military applications. For example, the protective shells of nuclear power plants are expected to survive the impact loading of an incoming missile or other sources; airport runways must withstand repeated dynamic loads due to aircraft take off and landing; dynamic loading on concrete structures or buildings arising from natural hazards (such as tornadoes, earthquakes and ocean waves) and

WIT Transactions on the Built Environment, Vol 98, © 2008 WIT Press
www.witpress.com, ISSN 1743-3509 (on-line)
doi:10.2495/SU080251

accidental impact or deliberate explosion is also of great practical concern. Characterization of the behavior of concrete under impact or impulsive loading is a prerequisite for the design and analysis of these structures.

Several techniques have been developed to study the dynamic mechanical properties of concrete and concrete structures. For instance, a modified Charpy impact test [1], as in the conventional Charpy impact machine used by the metallurgists, where a swinging pendulum is allowed to strike a specimen in its path thereby transferring momentum and causing high stress rates. Other significant impact tests include the split Hopkinson pressure bar test [2, 3], in which the specimen is sandwiched between two elastic pressure bars and stress waves are generated by using a drop weight or a projectile. Two techniques mentioned above are not convenient for testing the impact resistance of reinforced concrete or concrete structures owing to the dimensions of the sample, thus, a drop weight impact test is always used to study the impact response of the concrete structures [4–10].

In the paper, a new drop weight impact machine has been specifically designed for dynamic tests, and also some impact tests were conducted on a high strength concrete. The explanations to the key phenomena are proposed.

This paper is structured as follows, the description of the machine is given in section 2, and detailed information for dynamic three-point bending tests is presented in section 3. In section 4 the results are presented and discussed, and finally, some conclusions are drawn.

2 Description of the drop weight impact machine

The schematic diagram of the drop weight impact machine is shown in Fig. 1. The machine is located inside the visible strong floor of the laboratory of Materials and Structures of the ETSI Caminos C. y P. of Ciudad Real. The two columns that guide the hammer are prestressed against the upper and lower 1 m-thick slabs of the strong floor, their height being 3.7 m. The columns push the lower slab of the strong floor through a 95 mm-thick steel plate to which the supports for the specimens can be attached. Between the steel plate and the concrete floor we put a very thin neoprene layer so as to distribute the stresses transmitted to the floor as uniformly as possible. In this way, the strong floor serves as a very stiff reaction frame; likewise, it is able to dissipate the energy transmitted through the specimen with negligible movement. Besides, the operation of the machine produces no damage or disturbance whatever to the structure of the building containing the lab, since the strong floor is a completely independent structure.

The frame supports two 90 mm diameter guide columns (rails), in which a hammer can be raised to a suitable height by a hoist and chain system, and then allowed to fall to impact samples supported on two supports as shown in Fig. 1.

The machine has the capability to provide a 2595 mm free drop height above the support. Two types of hammer were designed to fit for the tests on different types of specimens. One is the aluminium hammer with the mass 18.60 kg, the

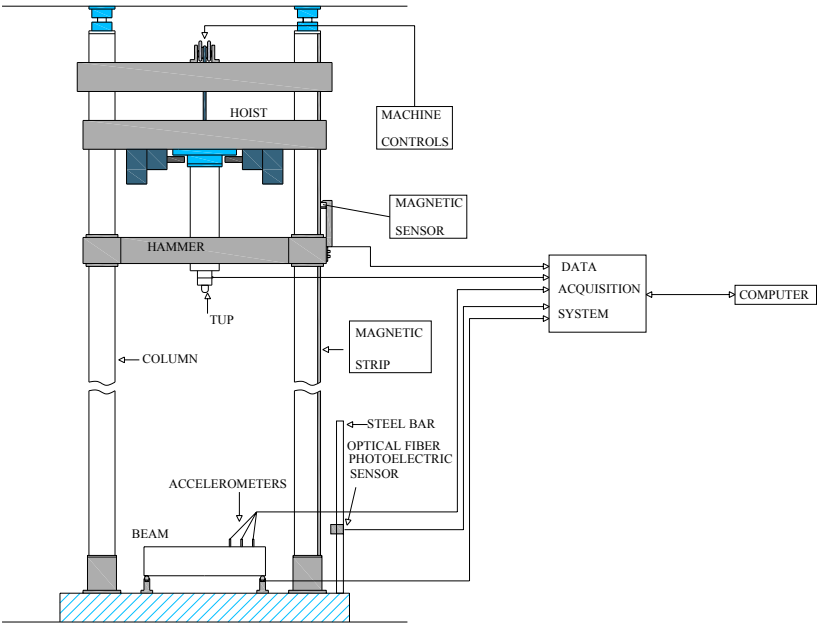

Figure 1: Schematic diagram of the drop weight impact machine.

other is the steel hammer, and the mass can be from 60.55 kg to 315.55 kg, the increment is 15 kg. By dropping the hammer through different height, the applied loading rate can be varied.

2.1 Instrumentation used

2.1.1 Force sensors

The impact force between the hammer tup and the specimen is measured by a piezoelectric force sensor (made by PCB Company), Model 204C, the measurement range is up to 177.92 kN. Moreover, the reaction force between the support and the specimen is determined by another two force sensors, Model 203B, with the maximum measurement 89 kN. The calibrations of the sensors were also supplied by the PCB Company, and the accuracy of sensors is 0.7 N.

2.1.2 Accelerometers

The accelerometers mounted along the length of the beam are also piezoelectric sensors, with a resonant frequency greater than 70 kHz. With a resolution of 0.1 g, the accelerometers can read up to ± 1000 g (where g is the Earth's gravitational acceleration). The calibrations of the accelerometers were supplied by the PCB Company.

2.1.3 Magnetic strip and magnetic sensor

The position of the hammer along the column can be detected by a magnetic strip mounted on the column and a magnetic sensor fixed on the side of the hammer (Model MSK 5000), with the resolution 0.001 mm.

2.1.4 Optical fibre photoelectric sensor

When a steel plate fixed on the hammer that slides along the column passes by the light route of the optical fibre photoelectric sensor (Model: OMRON E3x-NA), which is mounted on a steel bar fixed on the steel frame shown in Fig. 1, the sensor emits a 24 voltages signal, which is used to trigger the data acquisition system.

2.1.5 Data acquisition system

The data acquisition system consists of two Tektronix oscilloscopes (Model: TDS3014B), two signal conditioners (Model: 482A22), one HBM MGCplus device and a computer.

The signal conditioner is a four-channel, line -operated for sensor systems. This unit provides constant current excitation to the built-in sensor amplifier and decouples the AC signal from the DC bias voltage. The constant current output is from 2 to 20 mA.

HBM MGCplus device is used to acquire the data from the magnetic sensor, namely, the position of the hammer. The acceleration of the hammer can be obtained from the position versus time, and also the impact velocity can be determined.

The Tektronix oscilloscope has four channels to record the data from sensors during the impact process. The device has a bandwidth 100 MHz, maximum sample rate 1.25GHz.

3 Dynamic three-point bending tests

To investigate the effect of the loading rate on the fracture behaviour of the high strength concrete, three-point bending tests on notched beams were carried out as sketched in Fig. 1. The dimensions of the test beams were 100×100 mm in cross section, and 420 mm in total length. The initial notch-depth ratio was approximately 0.5, and the span was fixed at 400 mm during the test.

The drop height of the hammer was set 300 mm, the hammer acceleration was 9.62 m/s^2, and the impact velocity was 2.40 m/s. For the data acquisition system, the sample rate was set 1 MHz.

3.1 Material characterization

A single high strength concrete was used throughout the experiments, made with an andesite aggregate of 12 mm maximum size and ASTM type I cement. Microsilica fume slurry and superplasticizer (ACE 325, B225) were used in the concrete composition. The water to cement ratio (w/c) was fixed at 0.33.

There was a strict control of the specimen-making process, to minimize scattering in test results. All of the specimens were cast in steel molds, vibrated

by a vibrating table, wrap-cured for 24 hours, demolded, and stored for 4 weeks in a moist chamber at 20℃ and 98% relative humidity until they were tested.

Compressive tests were conducted according to ASTM C39 and C469 on 75 mm×150 mm (diameter × height) cylinders. Brazilian tests were also carried out using the same dimensional cylinders following the procedures recommended by ASTM C469. We made 8 cylinders, 4 for compression tests and 4 for splitting tests. Table 1 shows the characteristic mechanical parameters of the concrete determined in the various characterization and control tests. The mass density of the material is 2337.5 kg/m^3.

Table 1: Mechanical properties of the high strength concrete.

	f_c (MPa)	f_t (MPa)	E_c (GPa)
Mean	96.98	5.18	33.87
Std. Dev	5.91	0.44	1.20

3.2 Determination of the loading point displacement

There are several techniques to measure the loading point displacement under dynamic loading conditions. For example, a non-contact linear-proximity measuring system [7, 11], high speed camera [7, 12], accelerometers [4, 7]. Here, accelerometers were used to determine the loading point displacement.

Three accelerometers were mounted along the length of the beam as shown in Fig. 2, the distance between neighbours were 40 mm, and the left one (Position 1) was away from the centre of the specimen 80 mm. The displacement of position 1, 2 and 3 where accelerometers locate can be obtained by double integration of the acceleration, then, the loading point displacement can be determined by linear extrapolation.

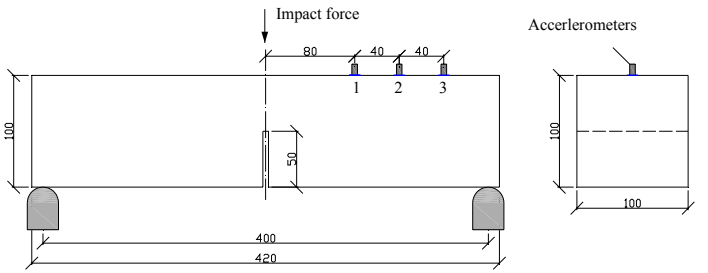

Figure 2: Geometry of specimen and positions of accelerometers.

4 Experimental results and discussion

Five impact tests were conducted using the drop weight impact machine, the typical results are presented as follows.

Fig. 3 shows a typical impact and reaction forces versus time curves, where the reaction force was evaluated by summing the values from both support data

points. The actual impact pulse is the first pulse, with amplitude of 40.24 kN, the later a smaller amplitude pulse is rebound of the tup, recorded after the specimen has already failed. The reason the impact force actually starts at approximately 0.01026 s and not zero is because the signal has not been time shifted.

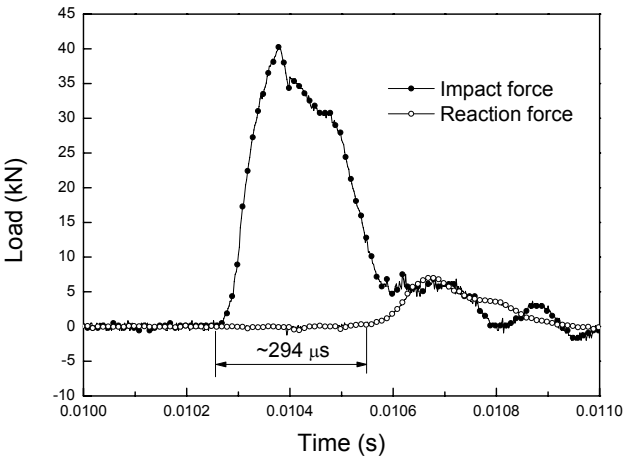

Figure 3: Typical impact and reaction forces versus time.

Comparing the impact force with the reaction force, it is obvious that the peak load of the impact force (40.24 kN) is much greater than that of the reaction force (7.06 kN), and the latter is only 17.5% of the former. This indicates that the most of the impact force is used to maintain the balance with the inertia force during loading, while only a small portion of the impact force is actually used to deform and fracture the specimen, its value equals the reaction force [4], thus, the reaction force was used to calculate the work of fracture under dynamic loading.

It is worth to note, the time interval is around 294 μs between the start points of the impact force and the reaction force. However, it only takes approximately 59 μs for the longitudinal stress wave travels from the impact point to the support point. Thus, there is an apparent time delay, this time delay was also found in reference [13], even though the vertical movement of the reinforced beam was restrained using two steel yokes. The reason for this time delay can be explained as follows. Although the specimen begins to be loaded by the impact pulse as it reaches the specimen, the amplitude of its initial rise period is too small to enable the specimen to deform sufficiently so that variations in the contact resistance are generated. As such, the signal of the reaction force does not show an obvious variation during this initial loading period. However, when the impact energy absorbed by the specimen is large enough, a measurable signal variation begins due to the relatively great changes in contact resistance caused by the specimen deformation.

Fig. 4 shows the displacement of different positions along the beam versus time; the loading point displacement was obtained by linear extrapolation according to the displacement of position 1, 2 and 3.

Fig.5 shows the impact and the reaction forces versus time curves, the initial time of the reaction force has been shifted, thus, the impact and the reaction forces have the same starting points. The energy consumed by the specimen is determined by the area under the load-displacement curves. It is clear that most of the impact energy (9.91 J) absorbed by the beam is used to maintain the balance with the kinetic energy, strain energy and also some energy absorbed by the elastic deformation of the machine. Only a small portion of the impact energy, work of fracture (1.3 J) is used to deform and fracture the beam, this energy represents the energy required to create two new fracture surfaces. In this case, the total energy provided by the hammer is 53.57 J.

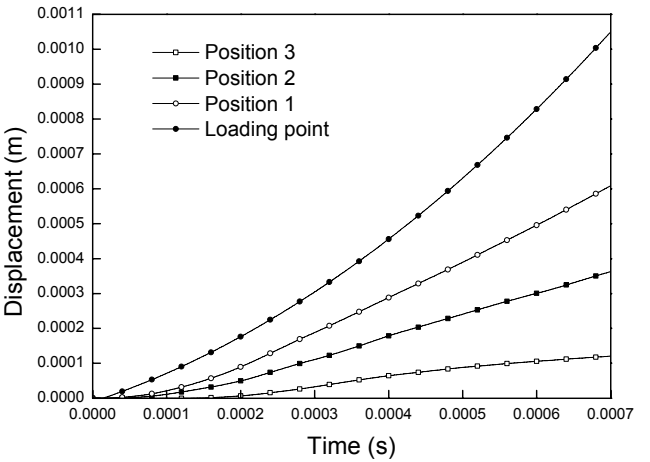

Figure 4: Displacement versus time.

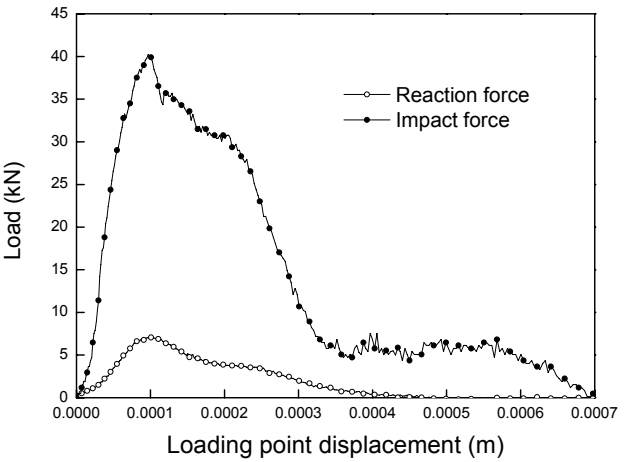

Figure 5: Load versus displacement.

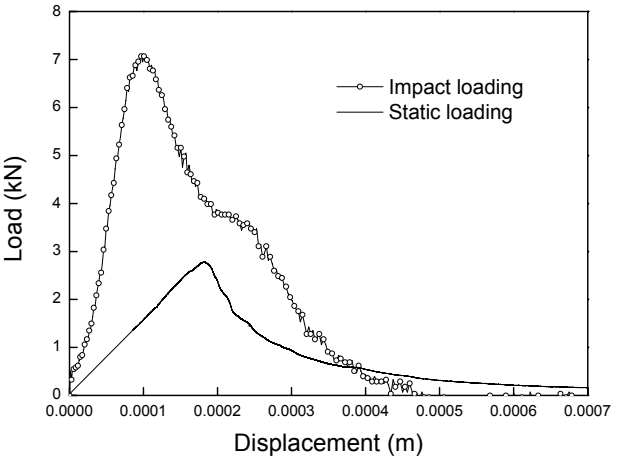

Figure 6: Comparison of load versus displacement.

Fig. 6 presents a comparison between the reaction force under impact loading and the bending load under static loading conditions. The static tests corresponded to a crosshead movement rate of 1.74×10^{-8} m/s. The reaction force was adopted as the impact results, and also was used to calculate the work of fracture under impact loading as presented before. The work of fracture (1.3 J) under impact loading is much higher than that (0.7 J) under static loading; the significant loading rate sensitivity can be noticed. The concrete is stronger (high peak load) and tougher (more work of fracture) under impact loading than under static loading conditions. This tendency on high strength concrete is in accordance with the results obtained by other researchers [4, 14].

5 Conclusions

A new drop weight impact machine is successfully made to investigate the impact behaviour of concrete and concrete structures.

The time delay during the test between the impact force and the reaction force is due to it takes some time for the relatively great changes in contact resistance caused by the specimen deformation.

Most of the impact force is used to maintain the balance with the inertia force, and only a small portion of the impact force is actually used to deform and fracture the specimen.

The high strength concrete is a loading rate sensitivity material, it resists higher load and absorbs more energy under impact loading than under static loading.

Acknowledgements

We acknowledge financial support for this research from Ministerio de Educación y Ciencia, Spain, under grants MAT 2006-356, and from OHL S.A. through research project O11.41781.

References

[1] Al-Oraimi S.K. & Seibi A.C., Mechanical characterisation and impact behaviour of concrete reinforced with natural fibres. *Composite Structures*, **32,** pp. 165–171, 1995.

[2] Grote D.L., Park S.W. & Zhou M., Dynamic behavior of concrete at high strain rates and pressures: I. Experimental characterization. *International Journal of Impact Engineering*, **25**, pp. 869–886,2001.

[3] Weerheijm J., *Concrete under impact tensile loading and lateral compression*, PhD Thesis, Delft University of Technology, 1992.

[4] Banthia N., Mindess S., Bentur A. & Pigeon M., Impact testing of concrete using a drop-weight impact machine. *Experimental Mechanics*, **29,** pp. 63–69, 1989.

[5] Banthia N. & Mani M., Toughness indices of steel fiber reinforced concrete at subzero temperatures. *Cement and Concrete Research*, **23,** pp. 863–873, 1993.

[6] Banthia N., Mindess S. & Trottier J.F., Impact resistance of steel fiber reinforced concrete. *ACI Materials Journal*, **93**, pp. 472–479, 1996.

[7] Banthia N., Yan C. & Sakai K., Impact resistance of fiber reinforced concrete at subnormal temperatures. *Cement and Concrete Composites*, **20,** pp. 393–404, 1998.

[8] Bindiganavile V. & Banthia N., Size effects and the dynamic response of plain concrete. *Journal of Materials in Civil Engineering*, **18,** pp. 485–491, 2006.

[9] May I.M., Chen Y., Roger D., Owen J., Feng Y.T. & Thiele P.J., Reinforced concrete beams under drop-weight impact loads. *Computers and Concrete*, **3**, pp. 79–90, 2006.

[10] Kishi N., Mikami H., Matsuoka K.G. & Ando T., Impact behavior of shear-failure-type RC beams without shear rebar. *International Journal of Impact Engineering*, **27**, pp. 955–968, 2002.

[11] Jerome D.M. & Ross C.A., Simulation of the dynamic response of concrete beams externally reinforced with carbon-fiber reinforced plastic. *Computers and Structures*, **64**, pp.1129–1153, 1997.

[12] Hughes B.P. & Al-Dafiry H., Impact energy absorption at contact zone and supports of reinforced plain and fibrous concrete beams. *Construction and Building Materials*, **9**, pp. 239–244, 1995.

[13] Soleimani S.M., Banthia N. & Mindess S., Behavior of RC beams under impact loading: Some new findings. *Proc. 6th International Conference on Fracture Mechanics of Concrete and Concrete structures*, eds. A. Carpinteri, P. Gambarova, G. Ferro & G. A. Plizzari, Taylor & Francis: Italy, Catania, pp. 867–874, 2007.

[14] Schuler H., Mayrhofer C. & Thoma K., Spall experiments for the measurement of the tensile strength and fracture energy of concrete at high strain rates. *International Journal of Impact Engineering*, **32**, pp. 1635–1650, 2006.